

# Crystallization and preliminary crystallographic analysis of a new class of glutathione transferase from nematodes

I. A. Kriksunov,<sup>a</sup> D. J. Schuller,<sup>a</sup>  
A. M. Campbell,<sup>b</sup> J. Barrett,<sup>b</sup>  
P. M. Brophy<sup>b</sup> and Q. Hao<sup>a\*</sup>

<sup>a</sup>MacCHESS at Cornell High Energy Synchrotron Source, Cornell University, Ithaca, NY 14853-8001, USA, and <sup>b</sup>Institute of Biological Sciences, University of Wales, Aberystwyth SY23 3DA, Ceredigion, Wales

Correspondence e-mail: qh22@cornell.edu

Mouse and *Heligmosomoides polygyrus* constitute a readily manipulated small-animal laboratory model for investigating host–nematode interactions. Two major forms of glutathione transferase (GST) are expressed in *H. polygyrus* adult worms following primary infection. One of these forms belongs to a new class of GST which has only been found in the nematode phylum and therefore presents a possible target for nematode control. In this study, crystals were obtained of a recombinant representative of this new GST class from *H. polygyrus*. These crystals belong to the triclinic space group *P*1, with unit-cell parameters  $a = 72.7$ ,  $b = 74.0$ ,  $c = 88.6$  Å,  $\alpha = 79.1$ ,  $\beta = 80.1$ ,  $\gamma = 81.5^\circ$ , and are likely to contain four homodimers in the asymmetric unit. X-ray diffraction data were collected to 1.8 Å resolution on station A1 at the Cornell High-Energy Synchrotron Source (CHESS).

Received 12 November 2002

Accepted 22 April 2003

## 1. Introduction

Parasitic nematodes are one of the most important limitations to intensive livestock production worldwide, with resistance to chemotherapeutics on the verge of a crisis (Waller, 1997; Sangster, 1999; Geary, 1999). An understanding of nematode xenobiotic metabolism is necessary to optimize chemotherapeutic efficacy and ultimately counteract resistance in the likely absence of new drug classes (Waller, 1997). The overall activity of the major phase II detoxification system in adult nematodes, glutathione transferase (GST), has been correlated with drug efficacy and resistance (reviewed in Brophy & Pritchard, 1994). Mouse and the strongylid nematode *Heligmosomoides polygyrus* comprise a convenient laboratory model for investigating host–nematode interactions (Finkelman, 1997). Mice are small animals, conditions for their laboratory culture are well known and techniques for genetic and other manipulation are well established. Information gained from this laboratory model could easily be transferred to economically important animals.

The soluble GST superfamily consists of multifunctional dimeric proteins involved in the detoxification of endogenous and xenobiotic compounds. Specific GSTs may also have ‘housekeeping’ molecular functions in the binding and transport of hydrophobic ligands, leukotriene synthesis and amino-acid catabolism (reviewed in Salinas & Wong, 1999). Cellular physiological roles have been predicted for GSTs as components of stress-

related cellular signaling pathways that lead to apoptosis. As a likely consequence of these diverse molecular and cellular roles, organisms usually express multiple forms of GST.

Seven phylogenetically widespread classes of soluble GST have been proposed:  $\alpha$ ,  $\mu$ ,  $\pi$ ,  $\theta$ ,  $\sigma$ ,  $\zeta$  and  $\omega$  (Mannervik *et al.*, 1985; Board *et al.*, 1997, 2000; Edwards *et al.*, 2000). Some bacteria express a  $\beta$ -class GST (Vuilleumier, 1997) and higher invertebrates a  $\delta$ -class GST (Zhou & Syvanen, 1997). Only  $\varphi$  and  $\tau$  classes of GST have been associated with plants (Edwards *et al.*, 2000). The assortment of GSTs may differ in particular organisms, species or phyla. Within each proposed GST class there is greater than 60% amino-acid sequence identity, whereas between classes there is only ~20–30% identity.

*H. polygyrus* adult worms express two major forms of GST following primary infection (Brophy, Bensmith *et al.*, 1994; Campbell *et al.*, 2001). One of these forms belongs to a recently discovered class of GST which has only been seen in the nematode phylum (Campbell *et al.*, 2001). This new class includes multiple GSTs from the genome-verified free-living nematode *Caenorhabditis elegans* as well as additional members found in parasitic nematodes from domesticated animals (Van Rossum *et al.*, 2001). Since this new class of GST appears in nematodes but not in their hosts, it presents a possible target for nematode control if specific inhibitors can be developed. No X-ray structures exist for members of this GST class and the low sequence identity with other GST classes diminishes the possible usefulness of homology modeling in the rational develop-

ment of inhibitors, which requires detailed knowledge of the active site. With the goal of completing a structure for a nematode-class GST, we report the crystallization and preliminary characterization of diffraction from a recombinant representative of this new class of GST from *H. polygyrus*.

## 2. Expression and purification

Recombinant *H. polygyrus* GST-2 (rHpolGST2) was expressed in *Escherichia coli* BL21 DE3 pLysS using the pET23d expression vector (Novagen), purified by glutathione affinity chromatography and enzymatically analyzed as described previously (Campbell *et al.*, 2001). SDS-PAGE and Western blotting were performed based on the methods described by Sambrook *et al.* (1989). Polyclonal antibodies were raised against the recombinant rHpolGST2 (Genosphere Biotechnologies, Antibodies Service, 2 Rue des Gravilliers, 75003 Paris, France). The mouse–nematode system for Western blot testing was maintained by standard procedures (Brophy *et al.*, 1995).

Batches of rHpolGST2 prepared for crystallographic analysis were first analyzed for purity by SDS-PAGE (Fig. 1) and confirmation that this recombinant form was expressed in native nematode tissues was demonstrated by Western blot analysis. The

integrity of rHpolGST2 was analyzed using a Micromass QToF-2 electrospray ionization quadrupole time-of-flight mass spectrometer (ESI QTOF-MS). The peak displayed a size of 23 389.78 Da representing the true weight of the pure protein, compared with the weight of 23 387.68 Da predicted using the *BioEdit* program (Hall, 1999).

## 3. Crystallization

rHpolGST2 samples were eluted in 0.05 M Tris–HCl pH 8.8 containing 0.015 M glutathione (GSH) and stored at 193 K. For crystallization purpose, the protein sample was thawed and dialyzed with 0.05 M Tris–HCl pH 8.5 buffer to eliminate GSH and to concentrate the sample to  $\sim 5 \text{ mg ml}^{-1}$ .

A fine grid of conditions derived from the initial crystallization screen (Jena Bioscience, Germany) was explored, with variables including pH, precipitant concentration and additives. Final crystals were grown using the hanging-drop method by mixing 1  $\mu\text{l}$  of rHpolGST2 protein with 1  $\mu\text{l}$  of reservoir solution containing 12% polyethylene glycol (PEG) 20K, 0.05 M CaCl<sub>2</sub> and 0.1 M Tris–HCl pH 8.5. Drops with the above conditions did not produce any crystals at room temperature for 3 d, after which they were moved to an incubator at 292 K. Overnight, crystals in a cluster grew to approximately 100  $\times$  100  $\times$  600  $\mu\text{m}$  in size (Fig. 2).

**Table 1**

Data-collection statistics.

Values in parentheses refer to the last resolution shell (1.86–1.80 Å).	
Space group	<i>P</i> 1
Unit-cell parameters (Å, °)	$a = 72.7$ , $b = 74.0$ , $c = 88.6$ , $\alpha = 79.1$ , $\beta = 80.1$ , $\gamma = 81.5$
Resolution range (Å)	25.0–1.8
Unique reflections	157158
$I/\sigma(I)$	13.1 (3.7)
$R_{\text{merge}}$ (%)	6.6 (32)
Completeness (%)	97.7
Multiplicity	6.9
Probable solvent content (%)	49

## 4. Data collection and analysis

Crystals were soaked in cryoprotection solution for a few seconds before freezing in a nitrogen cold stream at 100 K. The cryoprotection solution contained 85% crystallization precipitant (12% PEG 20K, 0.05 M CaCl<sub>2</sub>, 0.1 M Tris–HCl pH 8.5) and 15% glycerol. X-ray diffraction data were collected to 1.8 Å resolution on station A1 at the Cornell High-Energy Synchrotron Source (CHESS). The data were recorded using a Quantum 210 CCD detector (Area Detector Systems Co., CA, USA). The crystal-to-detector distance was 170 mm with a wavelength of 0.945 Å. A total of 720 images were taken with 1° oscillations. *DENZO/SCALEPACK* (Otwinowski & Minor, 1997) were used to process and reduce the data.

## 5. Results and discussion

The crystals have the symmetry of space group *P*1 and unit-cell parameters  $a = 72.7$ ,  $b = 74.0$ ,  $c = 88.6$  Å,  $\alpha = 79.1$ ,  $\beta = 80.1$ ,  $\gamma = 81.5^\circ$ . Assuming the presence of four homodimers in the asymmetric unit, a reasonable value for the Matthews coeffi-

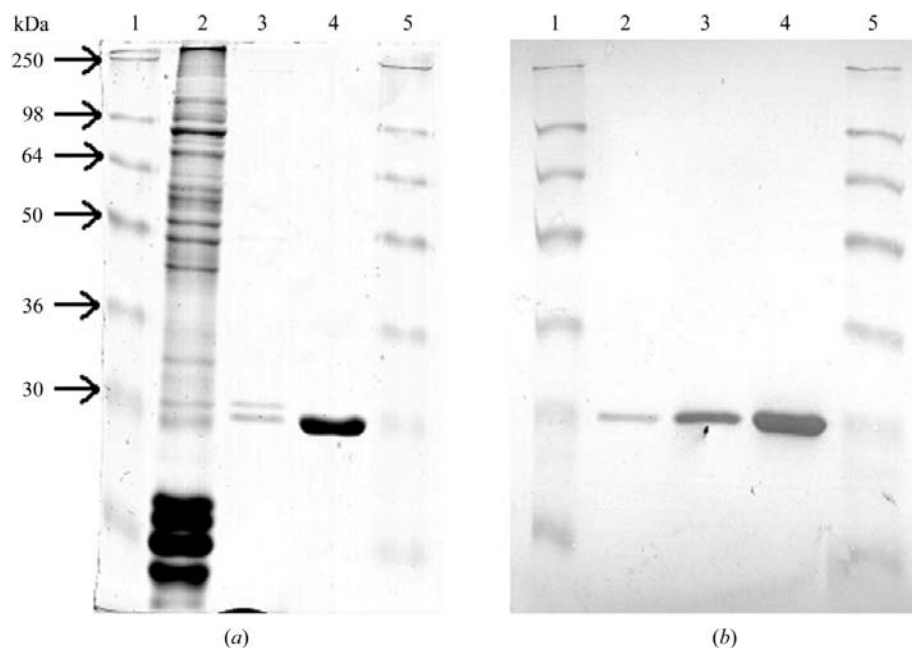


**Figure 1**

12.5% SDS-PAGE gel (a) and corresponding Western Blot (b) probed with rHpolGST2 polyclonal antibody. Lanes 1 and 5 contain SeeBlue pre-stained molecular-weight markers (Novex). Lane 2, adult somatic *H. polygyrus* extract. Lane 3, native glutathione affinity purified *H. polygyrus* GSTs. Lane 4, glutathione affinity purified rHpolGST2. The rHpolGST2 antibody recognizes a single specific product in adult *H. polygyrus* somatic extract, the native ‘nematode-specific type’ *H. polygyrus* GST2 as opposed to ‘the  $\alpha$ -type’ *H. polygyrus* GST1 (Brophy, Brown *et al.*, 1994) and the purified rHpolGST2 protein.



**Figure 2**

*H. polygyrus* GST2 crystal with dimensions of 100  $\times$  100  $\times$  600  $\mu\text{m}$ .

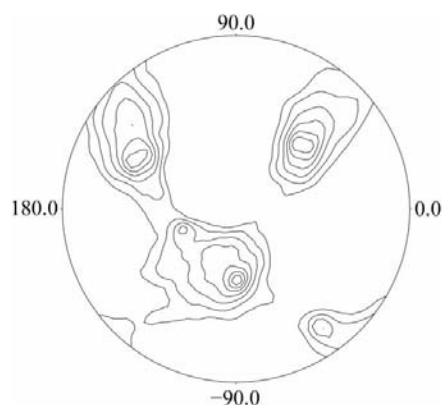


**Figure 3**  
Self-rotation function of rHpolGST2 calculated with data in the resolution range 15.0–2.5 Å and a Patterson radius of 18 Å. Only the  $\kappa = 180^\circ$  section of the map is shown; no significant features were seen in other portions of the map. The map was calculated with the CCP4 program POLARRFN (Collaborative Computational Project, Number 4, 1994).

cient of  $2.45 \text{ \AA}^3 \text{ Da}^{-1}$  is obtained, which corresponds to a solvent content of  $\sim 49\%$ . The likelihood of this is supported by evidence of 222 symmetry in the self-rotation function, which indicates that the asymmetric unit contents probably contain a multiple of four monomers (Fig. 3). Details of the data-collection and reduction statistics are shown in Table 1.

The molecular-replacement method will be used to attempt determination of the rHpolGST2 structure. Coordinates are available of numerous GSTs from other

classes, which might serve as search models for the molecular replacement, but none share more than 32% sequence identity with rHpolGST2.

A crystal structure of rHpolGST2 will contribute to the rational design of class-specific GST inhibitors. A structure will also increase understanding of the mechanisms of GST folding, catalysis and ligand binding.

The authors would like to thank BBSRC, UK for funding this research and also Mr Jim Heald and Mr Russell Morphew for the ESI QTOF-MS work and expert technical advice. This work is based upon research conducted at the Cornell High Energy Synchrotron Source (CHESS), which is supported by the National Science Foundation under award DMR 97-13424, using the Macromolecular Diffraction at CHESS (MacCHESS) facility, which is supported by award RR-01646 from the National Institutes of Health through its National Center for Research Resources.

## References

Board, P. G., Baker, R. T., Chelvanayagam, G. & Jermin, L. S. (1997). *Biochem. J.* **328**, 929–935.  
Board, P. G., Coggan, M., Chelvanayagam, G., Eastale, S., Jermin, L. S., Schulte, G. K., Danley, D. E., Hoth, L. R., Griffor, M. C., Kamath, A. V., Rosner, M. H., Chrnyk, B. A., Perregaux, D. E., Gabel, C. A., Geoghegan, K. F. & Pandit, J. (2000). *J. Biol. Chem.* **275**, 24798–24806.

Brophy, P. M., Bensmith, A., Brown, A., Behnke, J. & Pritchard, D. I. (1994). *Comp. Biochem. Physiol.* **109**, 585–592.  
Brophy, P. M., Bensmith, A., Brown, A., Behnke, J. & Pritchard, D. I. (1995). *Int. J. Parasitol.* **25**, 641–645.  
Brophy, P. M., Brown, A. & Pritchard, D. I. (1994). *Int. J. Parasitol.* **24**, 1059–1061.  
Brophy, P. M. & Pritchard, D. I. (1994). *Exp. Parasitol.* **79**, 89–96.  
Campbell, A. M., Teesdale-Spittle, P. H., Barrett, J., Jefferies, J. R. & Brophy, P. M. (2001). *Comp. Biochem. Physiol.* **128**, 701–708.  
Collaborative Computational Project, Number 4 (1994). *Acta Cryst.* **D50**, 760–763.  
Edwards, R., Dixon, D. P. & Walbot, V. (2000). *Trends Plant Sci.* **5**, 193–198.  
Finkelmann, F. D. (1997). *Annu. Rev. Immunol.* **15**, 505–533.  
Geary, T. G. (1999). *Int. J. Parasitol.* **29**, 105–112.  
Hall, T. A. (1999). *Nucleic Acids Symp. Ser.* **41**, 95–98.  
Mannervik, B., Ålin, P., Guthenberg, C., Jonsson, H., Tahir, M. K., Warholm, M. & Jornvall, H. (1985). *Proc. Natl Acad. Sci. USA*, **82**, 7202–7206.  
Otwinowski, Z. & Minor, W. (1997). *Methods Enzymol.* **276**, 307–326.  
Salinas, A. E. & Wong, M. G. (1999). *Curr. Med. Chem.* **6**, 279–309.  
Sambrook, J., Fritsch, E. F. & Maniatis, T. (1989). *Molecular Cloning: A Laboratory Manual*, 2nd ed. Cold Spring Harbor Laboratory Press.  
Sangster, N. C. (1999). *Int. J. Parasitol.* **29**, 115–124.  
Van Rossum, A. J., Jefferies, J. R., Young, C. J., Barrett, J., Tait, A. & Brophy, P. M. (2001). *Chem. Biol. Interact.* **133**, 274–277.  
Vuilleumier, S. (1997). *J. Bacteriol.* **179**, 1431–1441.  
Waller, P. J. (1997). *Vet. Parasitol.* **72**, 391–405.  
Zhou, Z. H. & Syvanen, M. (1997). *Mol. Gen. Genet.* **256**, 187–194.